

Crystal structure and anticonvulsant activity of (\pm)-1,2:4,5-di-*O*-isopropylidene-3,6-di-*O*-(2-propylpentanoyl)-*myo*-inositol

Sung C. Moon,^a Gustavo A. Echeverría,^{b,c,*} Graciela Punte,^b Javier Ellena^d and Luis E. Bruno-Blanch^a

^a*Cátedra de Química Medicinal, Departamento de Ciencias Biológicas, Facultad de Ciencias Exactas, Universidad Nacional de La Plata, Calle 47 y 115 sh. B1900AVV, La Plata, Argentina*

^b*LANADI e IFLP, Departamento de Física, Facultad de Ciencias Exactas, Universidad Nacional de La Plata, CC 67, (1900) La Plata, Argentina*

^c*Facultad de Ingeniería, Universidad Nacional de La Plata, (1900) La Plata, Argentina*

^d*Instituto de Física São Carlos, USP, CP 369, CEP 13560-970, São Carlos, SP, Brazil*

Received 28 December 2006; received in revised form 1 May 2007; accepted 2 May 2007

Available online 16 May 2007

Abstract—The biological activity and crystal structure of (\pm)-1,2:4,5-di-*O*-isopropylidene-3,6-di-*O*-(2-propylpentanoyl)-*myo*-inositol have been investigated. This compound shows better anticonvulsant activity than valproic acid (VPA) in the MES test as measured in mice. Its structure, determined from single-crystal X-ray diffraction measurements, shows that the inositol ring deviates from the ideal chair conformation and that the two 2-propylpentanoyl groups are located on opposite ring positions. This molecular conformation lets carbonyl and hydroxyl oxygen atoms to be available for hydrogen-bonding interactions, hinders carbonyl carbon atoms, preventing metabolic enzymatic hydrolysis, and helps to rationalize the observed inactive profile in the PTZ test. The anti-convulsant activity profile suggests a mechanism different from that of VPA.
© 2007 Elsevier Ltd. All rights reserved.

Keywords: Diketal; Valproic acid; Anticonvulsant; X-ray diffraction

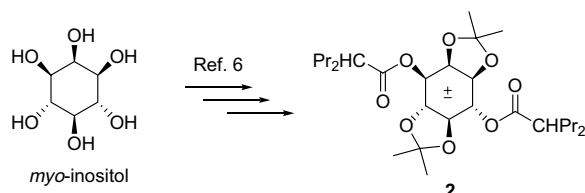
1. Introduction

Selectively protected *myo*-inositol chemistry has achieved intense interest since the recognition of the many biological implications of inositol. After the discovery in 1983 that inositol-1,4,5-trisphosphate [Ins(1,4,5)P₃] is a Ca²⁺-mobilizing second messenger,¹ a great effort was dedicated during the 1980s to the synthesis of inositol phosphates, some of which have shown to be components of cells. During the 1990s there followed an interest in the lipid phase, and this century has witnessed a renewed interest in the phosphate derivatives.² Diketals of *myo*-inositol are very important intermediates used to prepare the different inositol phosphate derivatives.³ One of the diketals more utilized is

the regioisomer (\pm)-1,2:4,5-di-*O*-isopropylidene-*myo*-inositol (**1**), and in our experience the best preparative technique for **1** is that described by Gigg and co-workers;⁴ however, this reaction proceeds to give a mixture of the diketals that cannot easily be separated. The functionalization of this mixture by O-acylation permits one to obtain a pure crystalline (\pm)-1,2:4,5-diketal derivative by a simple crystallization from the reaction medium.

Taking into account the anticonvulsant activity of the valproic acid (VPA)⁵ as well as its effectiveness in the localization of the central nervous system (CNS), the title compound has been synthesized within a more general project aimed to get derivatives of VPA with a more efficient therapeutic action. The synthetic procedure from **1** and 2-propylpentanoyl anhydride (Scheme 1) has been previously reported by some of us.⁶ The compound (\pm)-1,2:4,5-di-*O*-isopropylidene-3,6-di-*O*-(2-propylpentanoyl)-*myo*-inositol (**2**) was the major

* Corresponding author. Tel.: +54 221 424 6062x270; e-mail: geche@fisica.unlp.edu.ar



Scheme 1.

reaction product, which could be relatively easily isolated from the other derivatives.

It proves to have anticonvulsant action, but its profile differs from that of VPA. Therefore, to get an insight into the factors influencing the biological activity of the title compound, its crystal structure has been characterized by single-crystal X-ray diffraction.

2. Results and discussion

Figure 1 shows the molecular conformation and atom labeling. Significant intramolecular bond lengths, angles, and torsional angles are given in Table 1.

The *myo*-inositol ring adopts a distorted chair conformation. Although the mean C–C bond length and endocyclic C–C–C bond angles, 1.523(7) Å and 110.9(5)°, are close to those observed in the crystal of *myo*-inositol itself, 1.521(7) Å and 111(1)°, they have larger dispersion values, indicating a more strained inositol ring. On the contrary the mean ring C–C–C–C torsional angle

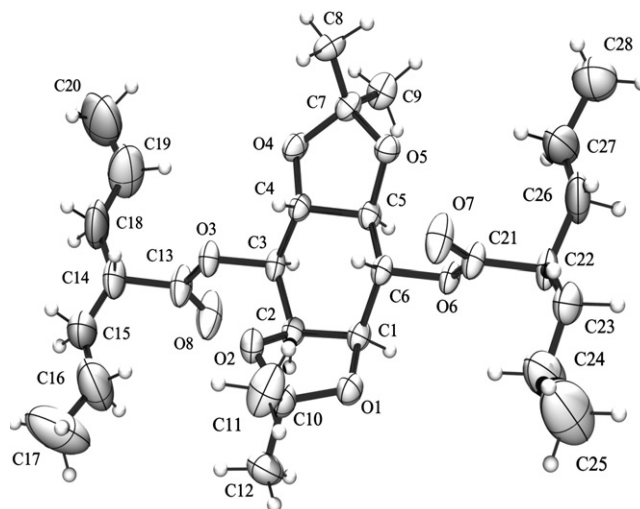


Figure 1. Ortep diagram of (±)-1,2:4,5-di-*O*-isopropylidene-3,6-di-*O*-(2-propylpentanoyl)-*myo*-inositol including the labeling scheme. Displacement ellipsoids are drawn at 50% probability.

52.7(7)° is smaller than the corresponding average C–C–C–C torsional angle value in *myo*-inositol, 56.8°,⁷ showing that ring strain is partially released by chair flattening. The ring flattening may be induced by the presence of the isopropylidene substituents in the 1,2- and 4,5-positions. According to Cremer and Pople⁸ the values of the ring puckering parameters, QT = 0.594(7) Å, $\theta = 154.4(7)^\circ$ and $\varphi = 52(1)^\circ$, show that the inositol ring distortion can be mainly described as a mixture of the chair and envelope conformers.

Table 1. Selected intramolecular bond distances (Å), bond angles (°), and torsional angles (°), e.s.d's in parentheses

<i>Inositol ring</i>					
C1–C2	1.558(6)	C1–O1	1.442(6)	C6–C1–C2	115.0(5)
C2–C3	1.532(6)	C2–O2	1.447(7)	C3–C2–C1	116.6(5)
C3–C4	1.483(6)	C3–O3	1.453(5)	C4–C3–C2	110.8(5)
C4–C5	1.505(6)	C4–O4	1.408(5)	C3–C4–C5	109.7(5)
C5–C6	1.499(6)	C5–O5	1.424(5)	C6–C5–C4	107.9(5)
C6–C1	1.536(6)	C6–O6	1.442(5)	C5–C6–C1	105.4(5)
C1–C2–C3–C4	−35.4(8)	C5–C6–C1–C2	−48.7(7)	O3–C3–C4–O4	−69.1(7)
C2–C3–C4–C5	54.4(7)	C6–C1–C2–C3	34.0(8)	O4–C4–C5–O5	41.0(6)
C3–C4–C5–C6	−74.8(6)	O1–C1–C2–O2	35.0(6)	O5–C5–C6–O6	−64.3(7)
C4–C5–C6–C1	68.3(6)	O2–C2–C3–O3	−42.0(6)	O6–C6–C1–O1	79.4(5)
<i>Valproate 1</i>					
O3–C13	1.309(8)	C18–C19	1.37(2)	C14–C15–C16	136(1)
O8–C13	1.221(8)	C19–C20	1.25(2)	C13–C14–C18	114(1)
C13–C14	1.49(1)	C3–O3–C13	118.9(6)	C14–C18–C19	134(1)
C14–C15	1.38(1)	O3–C13–C14	115.3(8)	C18–C19–C20	124(2)
C15–C16	1.31(2)	O8–C13–C14	123.6(8)	C14–C13–O3–C3	178.3(8)
C16–C17	1.39(1)	O3–C13–O8	121.1(7)	O3–C13–C14–C15	−95(1)
C14–C18	1.30(2)	C15–C16–C17	132(2)	O3–C13–C14–C18	88(1)
<i>Valproate 2</i>					
C21–O6	1.308(7)	C27–C28	1.461(9)	C22–C23–C24	117.3(8)
C21–O7	1.196(7)	C22–C26	1.45(1)	C21–C22–C26	108.9(7)
C21–C22	1.485(8)	C6–O6–C21	118.2(5)	C22–C26–C27	135(1)
C22–C23	1.520(8)	C22–C21–O6	113.6(7)	C26–C27–C28	133(1)
C23–C24	1.414(8)	C22–C21–O7	124.1(7)	C22–C21–O6–C6	−178.6(5)
C24–C25	1.48(1)	O6–C21–O7	122.2(6)	O6–C21–C22–C26	102.8(9)
C26–C27	1.186(9)	C23–C24–C25	119(1)	O6–C21–C22–C23	−138.1(7)

The valproate groups are equatorially bonded to opposite position of the *myo*-inositol ring through the hydroxylic oxygen. The O–C=O carboxylic plane locates approximately perpendicular to the mean *myo*-inositol and 2-propylpentanoyl plane (the angles are 69(1)° and 86(2)°, respectively) with the carbonyl group pointing outwards in opposite directions. Due to this molecular conformation, the carbonyl carbon is sterically hindered by the valproate group and the *myo*-inositol ring, while the carbonyl and hydroxyl oxygen atoms are not. Thus, the latter are available to establish hydrogen bonds with any proton-donor group of the surrounding molecules. In the present compound intramolecular C(ring)–H(axial)⋯O(carbonyl) hydrogen-bond type interactions are observed (see Table 2).

The pendant 2-propylpentanoyl groups adopt an almost planar conformation with one end somewhat displaced from the plane, causing the chains to extend to almost their maximum possible value (mean length is 7.137(3) Å).

As was suggested before, the therapeutic action of an anticonvulsant drug depends not only on its anticonvulsant activity, but also on its effectiveness in the localization in the CNS. Regarding **2** we expected that the passage through the blood–brain barrier (BBB) of this compound would be easier than in the case of VPA due to its higher hydrophobic properties, and we anticipated that when getting into CNS it would release VPA after metabolic enzymatic hydrolysis. To examine **2**'s anticonvulsant activity, maximal electroshock (MES) and pentylenetetrazol (PTZ) tests were employed (see Table 3). The observed effective dose in 50% of the tested mice (ED₅₀) for the MES test was 79.6 μmol/kg at the time of peak effect (TPE), which has been determined to be 1 h. In **2** the relative potency (RP) in the

MES test, defined as the ED_{50(VPA)}/ED₅₀₍₂₎, was found to be 12.7 times larger than in VPA. A difference from VPA is that **2** was inactive in the pentylenetetrazol (PTZ) test. It should be mentioned that when tried in the RotoRod test, **2** did not show acute toxicity up to doses of 450 μmol/kg. Contrary to our previous idea about the possible release of VPA from **2** after its metabolic enzymatic hydrolysis, the PTZ test results suggest an anticonvulsive activity mechanism different from that of VPA. Moreover, this finding seems to indicate that **2** acts as a drug with anticonvulsant activity by itself, since it is not likely that the metabolized substances, at the CNS, released the VPA group and produced a pharmacological action dissimilar from that of VPA. This hypothesis is supported by the molecular geometry, the observation that the carbonyl carbon is sterically hindered by both the valproate group and the *myo*-inositol ring also suggests that the molecules of **2** could not be easily hydrolyzed. Furthermore, the results of Armand et al.⁹ and Redecker et al.¹⁰ are in line with our findings. These authors suggested that other VPA sugar-alcohol esters analyzed by them do not represent prodrugs of VPA.

2.1. Conclusions

The comparison of MES and PTZ test results for **2** and VPA, along with the analysis of the molecular geometry in **2** that shows that there are steric impediments for metabolic enzymatic hydrolysis of the carbonyl carbon atoms, allows one to suggest that **2** presents an anticonvulsive activity mechanism that is different from that of VPA and to propose that **2** itself acts as a distinctly different drug with anticonvulsant activity.

3. Experimental

3.1. General

The melting point was determined on an Electrothermal IA6304 apparatus and is uncorrected. Analytical thin-

Table 2. Selected non-bonded contacts (Å) and angles (°), e.s.d's in parentheses

	D–H	H⋯A	D⋯A	D–H⋯A
C(5)–H(5)⋯O(7) ⁱ	0.98	2.43	3.331(8)	153
C(6)–H(6)⋯O(7)	0.98	2.24	2.640(7)	103

Symmetry codes: (i) $-x, -1/2 + y, -z$.

Table 3. Anticonvulsant activity of **2** (phase 2)^a

TPE ^b hours		MES		PTZ ^c		RotoRod	PI ^e	RP ^f
		ED ₅₀				TD ₅₀ ^d		
		μmol/kg	mg/kg	μmol/kg	mg/kg	μmol/kg		
2	1	79.6 (68.3–92.9)	40.8 (35.0–47.6)	0% at 450	0% at 230.4	0% at 450	>5.7	12.7
VPA ^g	0.25	1888 (1715–2347)	272.0 (247–338)	1035 (854–1229)	149.0 (123–177)	425.9 (369–450)	1.6	1

^a In parentheses are listed the intervals of the 95% confidence of the ED₅₀ tests (Ref. 23).

^b TPE: time peak effect according to the MES test.

^c The doses of **2** were intraperitoneally administered.

^d Corresponds to all analyzed periods of time.

^e PI (Protective Index) = (TD₅₀/ED₅₀) taking into account only the anticonvulsant potency against the MES test.

^f RP: see details in Section 2.

^g Ref. 24.

layer chromatography (TLC) was performed with 0.25-mm layer aluminum sheets Silica Gel 60 F-254 (E. Merck, Darmstadt, Germany). The spot was visualized with the sulfomolybdic reagent (with subsequent heating). The IR spectrum was recorded with a Perkin–Elmer 1600 FTIR spectrometer; the sample was examined as a pellet in KBr. NMR spectra were recorded on a Bruker AC-200 spectrometer. ^1H (200 MHz), and ^{13}C (50.2 MHz). Chemical shift are relative to Me_4Si ($\delta = 0.00$). FABMS was recorded on a Kratos MS80RFA (Kratos Analyticals, Manchester, UK) using a xenon beam of 8 kV.

3.2. Preparation of (\pm)-1,2:4,5-di-*O*-isopropylidene-3,6-di-*O*-(2-propylpentanoyl)-*myo*-inositol (**2**)

The synthesis of compound **2** was carried out, according to a procedure reported by us,⁶ mixing compound **1** (9.50 g, 36.5 mmol) with dry Et_3N (43 mL, 308 mmol) and 4-pyrrolidinopyridine (1.90 g, 12.8 mmol). Valproic anhydride (91.5 mmol) was added to the suspension at room temperature, under a dry nitrogen atmosphere. Details of the synthesis of **1** and purity testing are also reported in Ref. 6. The reaction mixture was stirred for 28 h with monitoring by TLC. After completion of the reaction, the solvent was evaporated under reduced pressure, the crude product was crystallized from MeOH to give **2** as white crystals (6.62 g, 12.93 mmol, 35.4%); R_f 0.72 (CH_2Cl_2); mp 143.5–145 °C; IR (KBr) cm^{-1} 1731 (C=O); ^1H NMR (CDCl_3): δ 5.29 (dd, 1H, J 11.1, 6.9 Hz, H-6), 5.12 (dd, 1H, J 10.6, 4.2 Hz, H-3), 4.58 (t, 1H, J 4.5 Hz, H-2), 4.13 (m, 2H, H-1, H-4), 3.45 (dd, 1H, J 11.1, 9.4 Hz, H-5), 2.55–2.35 (m, 2H, CH), 1.72–1.23 (m, 16H, CH_2), 1.56, 1.43, 1.38, 1.27 (4s, each 3H, 2CMe_2), 0.93, 0.90, 0.89, 0.86 (4s, 12H, 4 Me); ^{13}C NMR (CDCl_3): δ 176.1, 175.2 (2C, COO); 112.5, 110.2 (2C, CMe_2); 79.3, 76.5, 75.1, 74.8, 73.5, 70.2 (6C, inositol), 45.2, 44.9 (2C, CH), 34.5, 34.4, 34.1 (4C, overlapping signals, $\text{CH}_2\text{CH}_2\text{CH}_3$), 27.6, 26.8, 26.7, 25.7 (4C, CMe_2), 20.4, 20.3, 20.2, 20.1 (4C, $\text{CH}_2\text{CH}_2\text{CH}_3$), 13.9 (4C, overlapping signals, $\text{CH}_2\text{CH}_2\text{CH}_3$); FABMS: $[\text{M}+\text{Na}]^+$ Calcd, 535.6; found m/z 535.6; Anal. Calcd for $\text{C}_{28}\text{H}_{48}\text{O}_8$: C, 65.60; H, 9.44. Found: C, 65.36; H, 9.60.

3.3. X-ray data for (\pm)-1,2:4,5-di-*O*-isopropylidene-3,6-di-*O*-(2-propylpentanoyl)-*myo*-inositol (**2**)

It was found that good-quality single crystals of **2** could be obtained by slow evaporation from a methanol solution. Single-crystal X-ray data were taken on an automatic four-circle Enraf–Nonius CAD-4 diffractometer with graphite monochromated $\text{Cu K}\alpha$ ($\lambda = 1.54184 \text{ \AA}$) radiation. Crystals belong to the monoclinic system, space group $P2_1$, with two molecules per unit cell. Unit cell parameters and the orientation matrix for data

collection were obtained from a least-squares refinement using the setting angles of 25 reflections in the θ range 10–30°. Data were collected at room temperature [293(2) K] in the ω – 2θ scan mode up to $\theta_{\text{max}} = 35^\circ$, with a scan rate ranging 6.7–20° min^{-1} . Crystal data, additional details of data collection, and structure refinement are given in Table 4. One standard reflection measured every 30 min was used to apply a decay correction (the maximum decay was 1%). The data collection and reduction were performed with the programs CAD-4¹¹ and XCAD-4,¹² respectively.

The structure was solved by direct methods with SHELXS-86.¹³ The model was refined by full-matrix least-squares on F^2 by means of SHELXL-97.¹⁴ All the hydrogen atoms were stereochemically positioned and refined with the riding model.¹⁴ Once the complete isotropic model was obtained, an empirical absorption correction¹⁵ was applied (minimum and maximum transmission factors were 0.91221 and 0.94829, respectively), after which all non-H atoms were refined anisotropically. The hydrogen atoms were set isotropic with a thermal parameter 20% greater than the equivalent isotropic displacement parameter of the carbon atom to which each one was bonded. The refinement converged to $R_1 = 0.0549$ and $wR_2 = 0.0959$, with a goodness-of-fit on F^2 , $S = 1.405$ for 1338 observed reflections

Table 4. Crystal data, structure determination, and refinement summary

Empirical formula	$\text{C}_{28}\text{H}_{48}\text{O}_8$
Formula weight	512.66
Temperature (K)	293(2)
λ [Mo($\text{K}\alpha$)] (\AA)	1.54184
Crystal system	Monoclinic
Space group	$P2_1$
a (\AA)	10.735(3)
b (\AA)	9.667(3)
c (\AA)	15.681(3)
α (°)	90.0
β (°)	104.85(2)
γ (°)	90.0
V (\AA^3)	1572.9(8)
ρ_{calc} (g/cm^3)	1.082
Z	2
μ [Mo($\text{K}\alpha$)] (mm^{-1})	0.633
$F(000)$	560
Crystal size (mm)	$0.25 \times 0.19 \times 0.15$
Theta range for data collection (°)	2.92–69.95
Limiting indices	$-1 \leq h \leq 13$ $-1 \leq k \leq 11$ $-19 \leq l \leq 18$
Reflections collected/unique with $I > 2\sigma(I)$	3847/3348
Completeness to $\theta = 69.95$	95.7%
Goodness-of-fit on F^2	1.405
R	0.0549
R_w	0.0959
Absolute structure parameter	−0.7(4)
Extinction coefficient	0.00056(9)
$(\Delta/\rho)_{\text{max}}/(\Delta/\rho)_{\text{min}}$ ($\text{e}/\text{\AA}^{-3}$)	0.139/−0.153

[$I < 2\sigma(I)$] and 334 refined parameters. The atomic scattering factors were taken from the *International Tables for X-ray Crystallography*.¹⁶

The programs PLATON,¹⁷ PARST,¹⁸ and ORTEP-3¹⁹ were used within WINGX²⁰ for structure analysis and to prepare materials for publication. Atomic coordinates, bond lengths and angles, and thermal parameters have been deposited by the Cambridge Crystallographic Data Centre (No. CCDC 632662).

3.4. Biological activity

The pharmacological tests were performed according to standard procedures provided by the Antiepileptic Drug Development (ADD) Program of the National Institute of Neurological and Communicative Disorders and Stroke (NINCDS).²¹ Albino mice (N:NIH[S], weight: 18–25 g) were supplied by Facultad de Ciencias Veterinarias—Universidad Nacional de La Plata (Argentina). At the time of testing, the mice were used as experimental animals. Throughout the study, the animals were housed in colony cages on a 12 h light/dark cycle, and allowed free access to both commercial rodent chow and water ad libitum, except when they were removed from their cages and placed in individual ones for the experimental testing. Compound **2** was suspended in PEG 400. A volume of 3 mL/kg of the freshly made preparations was administered intraperitoneally (ip). The MES and PTZ tests were employed to determine the anticonvulsant activity (AC).

3.4.1. Anticonvulsant test. Maximal electroshock seizure test (MES test) was elicited in mice by delivering an electrical stimulus (50 mA; 60 Hz) for 0.2 s via ear electrodes. A drop of saline solution (0.9% sodium chloride solution) was applied to each ear before placing the electrodes to ensure adequate electrical contact. The animals were restrained by hand and released immediately after stimulation in order to permit observation of the seizure throughout its entire course. The maximal seizure typically consisted of a short period of tonic flexion followed by a longer period of tonic extension of the hind limbs and a final clonic episode. The tonic component was considered abolished if the hind limb tonic extension did not exceed an angle of 90° with the plane on the body;²² the absence of this component indicates that the test substance has the ability to prevent seizure spread. To determine the time of peak effect (TPE), four groups with four animals per group were employed. The animals for each group were intraperitoneally (ip) injected every 1/2, 1, 2, and 4 h and analyzed by the MES test. On the other hand, to evaluate the ED₅₀, four groups of eight animals were injected with different doses of **2**, and the effects were analyzed by the MES test at the TPE.

The PTZ tests identify substances that raise the seizure threshold. A freshly made solution of PTZ (1.7% in 0.9% sodium chloride solution) is administered subcutaneously (sc) into a loose fold of skin in the midline of the neck in a volume of 5 mL/kg body weight. This amount of PTZ induces convulsions in more than 97% of mice. To determine the TPE and the ED₅₀ parameters, we have used the procedure described previously. The animals were observed for at least 30 min after subcutaneous (sc) injection of PTZ for the presence or absence of a convulsive episode persisting for at least 5 s. Absence of a clonic seizure indicates protection.²²

3.4.2. Neurotoxicity tests. The RotoRod test was used exclusively in mice to assess minimal neurotoxicity. A normal mouse can maintain its equilibrium on a rotating rod (6 rpm) for long periods of time. Neurological deficit was indicated by failure to maintain balance on a rotating rod in each of three trials of 1 min each. Groups of eight animals per dose were injected and tested with the RotoRod test. The percentages of animals showing minimal neurotoxicity were recorded, and the higher dose producing neurotoxic effects was reported. TD₅₀ estimations could not be completed due to solubility problems with high doses.

Acknowledgements

G.P. and G.A.E. are members of the CONICET. The authors thank Comisión de Investigaciones Científicas de la Provincia de Buenos Aires (CICPBA), República Argentina, UNLP, and CSIC, Spain, for financial support. This research was supported in part through grants from Agencia de Promoción Científica y Tecnológica (PICT 06-11985/2004), CONICET, and Universidad Nacional de La Plata, Argentina. We thank to J. Dominguez-Cabrera from Cátedra de Química Medicinal, Facultad de Ciencias Exactas, Universidad Nacional de La Plata (Argentina) for carrying out the biological assays.

Supplementary data

Supplementary data associated with this article can be found, in the online version, at [doi:10.1016/j.carres.2007.05.004](https://doi.org/10.1016/j.carres.2007.05.004). Crystallographic data, excluding structure factors, have been deposited with the Cambridge Crystallographic Data Centre as supplementary publication with CCDC No. 632662. Copies of the data can be obtained free of charge on application with the Director, CCDC, 12 Union Road, Cambridge CB2 1EZ, UK (fax: +44 1223 336 033; e-mail: deposit@ccdc.cam.ac.uk).

References

1. Streb, H.; Irvine, R. F.; Berridge, M. J.; Schulz, I.. *Nature* **1983**, *306*, 67–69.
2. Irvine, R. F.; Schell, M. J. *Nat. Rev. Mol. Cell Biol.* **2001**, *2*, 327–338.
3. Chung, S.-K.; Chang, Y.-T.; Sohn, K.-H. *Chem. Commun. (Cambridge)* **1996**, 163–164.
4. Gigg, J.; Gigg, R.; Payne, S.; Conant, R. *Carbohydr Res.* **1985**, *142*, 132–134.
5. Löscher, W. *CNS Drugs* **2002**, *16*, 669–694, and references cited therein.
6. Bodor, N.; Moon, S. C.; Bruno-Blanch, L. *Pharmazie* **2000**, *55*, 184–186.
7. Rabinowitz, I. N.; Kraut, J. *Acta Crystallogr.* **1964**, *17*, 159–168.
8. Cremer, D.; Pople, J. A. *J. Am. Chem. Soc.* **1975**, *97*, 1354–1358.
9. Armand, V.; Louvel, J.; Pumain, R.; Ronco, G.; Villa, P. *Epilepsy Res.* **1995**, *22*, 185–192.
10. Redecker, C.; Altrup, U.; Hoppe, D.; Hense, T.; Kreier, A.; Rabe, A.; Dusing, R.; Speckmann, E. *J. Neuropharmacol.* **2000**, *39*, 267–281.
11. Enraf-Nonius. CAD-4-PC. Version 1.2. Enraf-Nonius: Delft, The Netherlands; 1993.
12. Harms, K.; Wocadlo, S. *XCAD-4. Program for Processing CAD-4 Diffractometer Data*; University of Marburg: Marburg, Germany, 1995.
13. Sheldrick, G. M. *SHELXS-86. Program for Crystal Structure Resolution*; Univ. of Göttingen: Göttingen, Germany, 1985.
14. Sheldrick, G. M. *SHELXL-97. Program for Crystal Structures Analysis*; Univ. of Göttingen: Göttingen, Germany, 1997.
15. Coppens, P.; Leiserowitz, L.; Rabinovich, D. *Acta Crystallogr.* **1965**, *18*, 1035–1038.
16. Wilson, A. J. C., Ed. *International Tables for Crystallography*; Kluwer Academic: Dordrecht, The Netherlands, 1995; Vol. C.
17. Spek, A. L. *Acta Crystallogr., Sect. A* **1990**, *46*, C34.
18. Nardelli, M. *PARST J. Appl. Crystallogr.* **1995**, *28*, 659.
19. Farrugia, L. J. ORTEP3 for Windows *J. Appl. Crystallogr.* **1997**, *30*, 565.
20. Farrugia, L. J. WinGX. An Integrate System of Windows Programs for the Solution, Refinement and Analysis of Single Crystal X-ray Diffraction Data. Dept. of Chemistry, University of Glasgow, 1997–2003.
21. Porter, M.; Cereghino, M.; Gladding, R.; Hessie, B.; Kupferberg, D.; Scoville, M.; White, D. *Cleveland Clinic. Quart.* **1984**, *51*, 293–305.
22. Chen, A.; Weston, J. K.; Bratton, A. C. *Epilepsia* **1963**, *4*, 66–76.
23. Litchfield, J. T.; Wilcoxon, F. *J. Pharmacol. Exp. Ther.* **1949**, *96*, 99–113.
24. Swinyard, E. A.; Woodhead, J. H.; White, H. S.; Franklin, M. R. Experimental Selection, Quantification, and Evaluation of Anticonvulsivants. In *Antiepileptic Drugs*, 3rd ed.; Levy, R., Dreifuss, F., Mattson, R., Meldrum, B., Penry, J., Eds.; Raven Press: New York, 1989; pp 85–102.